BioCore Exploring Scientific Community

International Journal of Nanotechnology in Medicine & Engineering

Research Article ISSN 2474-8811

Facile Bottom-up Approach to Synthesise Hydroxyapatite - Polymethyl Methacrylate Nanocomposites for Possible Applications in Bone Grafting

T. P. Gamagedara[1,2,3,*], R. M. G. Rajapakse[1,2]

[1]*Post Graduate Institute of Science, University of Peradeniya, Peradeniya, Sri Lanka*

[2]*Deparment of Chemistry, Faculty of Science, University of Peradeniya, Peradeniya, Sri Lanka*

[3]*Department of Basic Science, Faculty of Allied Health Sciences, University of Peradeniya, Peradeniya, Sri Lanka*

Abstract

Current applications of nanocomposites in medicine and surgery can be encouraged by using clinically well-known constituents in the preparation of nanocomposites. In addition, industrial production of medical devices made of nanocomposites can be increased by using simple one-pot methods. The process used in the study involves a bottom-up approach which starts with the synthesis of hydroxyapatite (HA) nanoparticles and polymethyl methacrylate (PMMA) simultaneously using basic precursors imitating strategies inside biological systems where it allows self-organizing into a higher order of microscale structure. In the present study, HA-PMMA nanocomposite was synthesized by a novel, facile bottom-up approach and its structural, morphological, mechanical and thermal properties were evaluated. X-ray diffractometry (XRD), Fourier transforms infrared (FTIR) spectroscopy, scanning electron microscopy (SEM), Thermo-gravimetric analysis (TGA) and differential scanning calorimetry (DSC) were used for the characterization. Homogeneous dispersion of needle shape, pure HA nanoparticles (~29% of HA) in the PMMA matrix can be obtained by a novel, one spot synthesis using $Ca(OH)_2$, $NH_4H_2PO^4$ precursors, MMA monomers and K_2S_2O8 initiator. The thermally and mechanically improved nanocomposite can be used for the possible applications in bone grafting with enough clinical and experimental data supporting the performance of HA nanoparticles and PMMA

Keywords: Hydroxyapatite, Polymethyl methacrylate, Nanocomposites, Self-assembly, Bone grafting

Corresponding author: **T. P. Gamagedara**

Dept of Basic Sciences, Faculty of Allied Health Sciences, University of Peradenya, Augusta Hill, Peradeniya, Sri Lanka

Email: tpiumnil@pdn.ac.lk

Citation: T.P.Gamagedara et al. (2019), Facile Bottom-up Approach to Synthesise Hydroxyapatite - Polymethyl Methacrylate Nanocomposites for Possible Applications in Bone Grafting. Int J Nano Med&Eng. 4:1, 1-8

Received: April 04, 2019

Accepted: April 17, 2019

Published: May 18, 2019

Introduction

Bone is a highly vascularized connective tissue that has a unique capability of spontaneous regeneration and to remodel its micro- and macrostructure [1]. Bone matrix is precisely composed of two major phases at the nanoscale level namely organic (polymer) phase and inorganic (mineral) phase. These phases have multiple components such as minerals, collagen, water, non-collagenous proteins, lipids, vascular elements and cells [2]. Here, the polymer, collagen acts as a structural framework in which plate-like tiny crystals of HA (4 nm x 50 nm x 50 nm) are embedded to strengthen the bone [3–8].

The structural and compositional strategies, by which they are precisely built, make bone an amazing and a true nanocomposite. Nature has built extremely hard and tough bone using such soft (collagen) and brittle (HA) ingredients. It is believed that key to the strength of the bone is the complex structural hierarchy into which it is organized in a self-assembling mode [3]. Molecular self-assembly is the assembly of molecules without guidance or management from an outside source [9]. Self-assembly can occur spontaneously in nature, for example, in cells and other biological systems, as well as in human engineered systems. At the nanostructural scale, biomineralization implies the molecular building of specific and self-assembled supramolecular organic systems which act as a previously arranged environment to control the formation of finely divided inorganic materials of approximately from 1 to 100 nm in size [10]. It usually results in an increase in internal organization of the system. Imitating these strategies, producing molecules with the ability to self-assemble into supramolecular assemblies is an important technique used in nanotechnology [9].

The broken bone is a lot more than painful and inconvenient, and mostly it is a costly and permanent health problem. According to the National Institutes of Health, approximately 1.5 million hip fractures occur worldwide each year, and this number might increase to 2.6 million by 2025 and 4.5 million by 2050[11]. Majority of fractures will heal well without the need for major intervention due to the high regeneration capacity of the bone, particularly in younger people [12,13]. However, many circumstances call for bone grafting owing to bone defects either from traumatic or from non-traumatic destruction such as tumours, infection, biochemical disorders, abnormal skeletal developments, etc [3,14]. There are multiple methodologies available for the treatment of bone defects, which include autografting,

allografting, xenografting and alloplastic or synthetic bone grafting [3]. The most commonly used bone grafts in the clinic are autologous and allogenic bone but there still exists some problems such as interaction, limited supply and allograft rejection. Apart from autologous and allogenic bone, alternative bone graft materials such as metals, polymers and ceramics are applied not only to fill the bone defects but also to provide mechanical and structural support [15]. One of the most important problems encountered in orthopaedic surgery is that the hardness of the bony metal or ceramic implant does not match each other. Nanodevices and nanomaterials interact with biological systems at atomic and molecular levels offer great advantages [16]. The strategy of incorporating of the bioactive component is still one of the most popular strategies to improve the mechanical strength, bioactivity and osteogenesis of polymer based scaffolds [15]. Due to its osseointegrative properties, nano-HA may represent a promising class of bone graft materials. It can form direct bonds with the host bone and it improves bone healing by stimulation of osteoblast activity and enhancing local growth factors [17].

Even though advanced researches have been carried out on many different types of nanocomposites, their use in medical devices is very much less than expected. One of the main reasons for lower usage of synthesized nanocomposites in clinical applications is that there is not enough reliable experimental and clinical data supporting the long-term performance of nanocomposites with respect to monolithic traditional materials [3,18].

This problem can be avoided by using clinically well-known constituents in the preparation of nanocomposites. Nano-scale HA has received much attention owing to its superior functional properties over its microscale counterpart. In addition, the in vitro and in vivo behaviour of nano-HA has extensively assessed in many studies and its biocompatibility was proven [17,19–22].

The properties of nano-HA can be improved with the aid of nanocomposites using biologically compatible polymers. [16] There is a major advantage of using synthetic polymers in the preparation of nanocomposites. Since the synthetic polymers can be produced under controlled conditions to exhibit predictable and reproducible mechanical and physical properties [3]. Long established use of PMMA cement provides the surgeon with satisfactory clinical data, whereas the newer systems have little to show in terms of clinical history [23,24]. PMMA used in bone cement is compliant and weak in comparison with natural bone; therefore, several reinforcement methods have been attempted [25,26]. The inclusion of bone particles in PMMA cement somewhat improves the stiffness and improves the fatigue life considerably [27]. The bone particles at the interface with patient's bone are ultimately resorbed and are replaced by ingrown new bone tissue [27].

A novel way of fabricating nanocomposite bone grafts using strategies found in nature has recently received much awareness and is recognized to be beneficial over conventional methods. As most of the methodologies of nanocomposite are not simple, it is of interest to find out a simpler method for the synthesis of nanocomposite for an orthopaedic application using clinically well-known substitutes such as HA and PMMA. In addition, PMMA is highly compatible with HA and it can also act as a functionalizing/linking material with HA [28]. Therefore, allowing nano-HA to self-assemble into PMMA matrix may enhance the mechanical properties of the composite. There are only a few earlier studies on HA-PMMA composites [23,29–32]. The process used in our study involves a bottom-up approach, which begins by synthesizing Nano-HA and PMMA using basic precursors simultaneously that have the ability to self assemble or self organize spontaneously into a higher order of microscale structure. According to the best of author's knowledge, there are no extensive studies on HA-PMMA nanocomposites. Therefore, in the present study HA-PMMA nanocomposites were synthesized by simple one-pot in-situ polymerization method and its structural, morphological, mechanical and thermal properties were evaluated.

Materials and Methods

Materials

All chemicals were of analytical grade and were used without further purification. Materials used in this synthesis were calcium hydroxide ($Ca(OH)_2$) powder, sodium persulphate ($Na_2S_2O_8$), ammonium dihydrogen orthophosphate ($NH_4H_2PO_4$), freshly distilled methyl methacrylate (MMA). De-ionized water is used throughout the experiment.

In situ synthesis of HA-PMMA Nanocomposites

First, 7.0 g (0.095 mol) of calcium hydroxide ($Ca(OH)_2$) powder was suspended in a 50 mL of a solution containing 1.0 g of sodium persulphate (Na_2S_2O8) dissolved in deionized water, in a round bottom three-necked flask. 6.8 g (0.059 mol) of ammonium dihydrogen orthophosphate ($NH_4H_2PO_4$) dissolved in 50 mL of deionized water and 10 mL (~ 0.1 mol) of freshly distilled methyl methacrylate were added drop-wise from two dropping funnels simultaneously to the suspension containing $Na_2S_2O_8$ and $Ca(OH)_2$ while maintaining the temperature at 80°C using a water bath and vigorously stirring with a magnetic stirrer. It was then refluxed at 80 °C for 2 hours. The molar ratio of Ca/P was maintained at 1.67. Water vapour from a steam generator was then passed into the emulsion until the polymer composite was coagulated. The PMMA-HA composite thus obtained was allowed to settle down and the supernatant was decanted. The residue obtained was washed with deionized water and the supernatant was decanted after allowing its residue to settle down. This was repeated for 2 more times and the residue was air dried for 24 hours. Finally, the sample was dried in a vacuum oven at 45°C and 600 mmHg.

Determination of the homogeneity of the nanocomposite

Randomly selected portions (~10 mg) of HAP-PMMA nanocomposite samples were heated to 30 – 500 °C at a rate of 5 °C min-1 using SCINCO STA N-1500 thermo-gravimetric analyzer for TGA and DSC analysis.

Determination of Mechanical Properties

Mechanical properties of the materials, such as the flexural strength (Modulus of Rupture, MOR), Young's Modulus (Y) were explored using a locally made universal mechanical testing machine with 4-point bending at a crosshead speed of 4.075 X 10^{-3} mms-1 (Fig. 1). In the case of 4-point bending, the MOR can be calculated according to the following equation (1):

$$MOR_{(4-point)} = \frac{3(l-a)P}{2bh^2} \qquad (1)$$

Where,

b, c, h - Dimensions of the bar [breadth, length, and height respectively]

a - Inner distance of the four-point bending setup (1 cm)

ℓ - Outer distance of the four-point bending setup (2 cm)

P - Force at breaking point

Young's Modulus (Y) was calculated by the following equation (2)

$$Y = \frac{Tensile\ Stress, \sigma}{Tensile\ Strain, \varepsilon} = \frac{s\,(l-a)P/2bh^2}{6hx/(1-a)(1+2a)} \qquad (2)$$

Where, x = depression at the load point.

2.5 Characterization techniques

X-ray diffraction (XRD) spectra were recorded using computer

controlled X-ray diffractometer (Seimens D 5000, Cu Kα radiation, λ = 0.1540562 nm, 18 kW rotating anode) (University of Peradeniya, Sri Lanka) and XRD analysis was done at 40 kV and 25 mA with a scanning rate of 10 min -1. For this study, powdered forms of the samples were used and Stainless steel was analyzed as it is. Particle size was obtained using the Debye-Scherer formulae (3).

$D=k\lambda/(\beta \cos\theta)$ (3)

Where;

D - Median size of the particle

K - Broadening constant (varying between 0.89 to 1.39)

λ - Wave length of Cu Kα radiation (λ = 1.54060 Å)

β - Full width at half maximum intensity (in radians) (FWHM)

θ - Position of peak maximum

Fourier Transform Infrared Spectroscopy (FTIR): The FTIR spectra were recorded using JASCO FTIR 410 spectrophotometer with 256 accumulations at 4 cm-1 resolution. 1 cm diameter constant-weight pellets (dispersed in KBr as pellets in the mass ratio of sample: KBr = 1:10) was used to record IR absorbance spectra.

Scanning Electronic Microscopic (SEM) studies were done by JEOL JSM-6320F Field Emission type scanning electron microscope (Shizuoka University, Japan), Hitachi SU6600 Analytical Variable Pressure Field Emission Scanning Electron Microscope (Shizuoka University, Japan) and ZEISS EVO LS15 Scanning Electron Microscope (University of Peradeniya, Sri Lanka). Samples were sputter-coated with gold by Quorum SE 7620 sputter coater (University of Peradeniya, Sri Lanka) before examination under the SEM.

Results and Discussion

X-Ray Diffraction (XRD)

Fig. 1 (a) shows the powder XRD patterns of pure HA prepared. The XRD pattern is comparable with the standard XRD pattern of pure HA (PDF # 74-0566), clearly showing the formation of HA from the synthetic procedure adopted in this work. The XRD pattern of the nanocomposite material also contains all the reflections corresponding to HA, indicating that the other components present in the reaction mixture do not disturb the HA formation reaction. In addition, all the XRD peaks of HA (Fig. 1b) are relatively broad, confirming the small size of HA nanoparticles in the nanocomposite. However, when the preparation of nanocomposites, the crystallinity of the HA phases was observed to be poorer according to Fig.1b, compared to that in pure HA. Intensities of two major peaks for (211) and (002) planes have been decreased due to the presence of polymer, indicating a reduction of the crystal growing energy of the inorganic crystals by the organic polymer. The average particle size was calculated from the XRD study using the Debye-Scherrer equation, along the c-axis (using (002) peak) and a-axis (using (310) peak) respectively, giving the dimensions of the HA crystals to be 23 nm and 17 nm in pure HA and 28 nm and 8 nm in HA-PMMA Nanocomposite. In the HA-PMMA Nanocomposite, the particle size of HA along the a-axis has reduced while the particle size along the c axis has slightly increased. PMMA may have a strong interaction with PO4 groups of HA which exposes in (010) plane. So that shielding effect by the polymer may control the growth along a-axis. Therefore, reduction of particle size along a-axis may be observed in the nanocomposite. In that case, dissimilarity of growth rates of (010) and (001) facets may lead to a needle shape rather than a spherical shape in the nanocomposite.

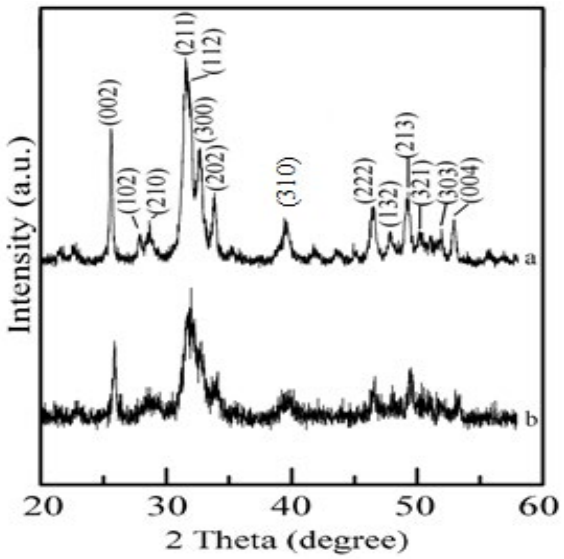

Fig.1: XRD pattern of (a) HA nanoparticles (H2) and (b) HA-PMMA Nanocomposite

Fourier Transform Infrared (FTIR) Spectroscopy

Fig. 2 shows the FT-IR spectra of pure HA (a), HA-PMMA nanocomposite (b), and pure PMMA (c) and expanded versions of the spectra in different wave number regions are shown in Figs. 3 - 6. The vibrations responsible for these bands are assigned in Table 1[33-37]. In the FT-IR spectrum of HA-PMMA nanocomposite, the band corresponding to ester carbonyl stretching vibration has been shifted to 1732 cm^{-1} from its position of 1734 cm^{-1} in pure PMMA and C=O band for PMMA is broader than the corresponding band for HA-PMMA (Fig 4) which suggests two different chemical environments at the C=O bond. In addition, vibration bands of C-O-C in the ester group at 1242 and 1269 cm^{-1} in pure PMMA were shifted to 1238 and 1271 cm^{-1} respectively in the nanocomposite, suggesting an interaction of PMMA and HA in the nanocomposite

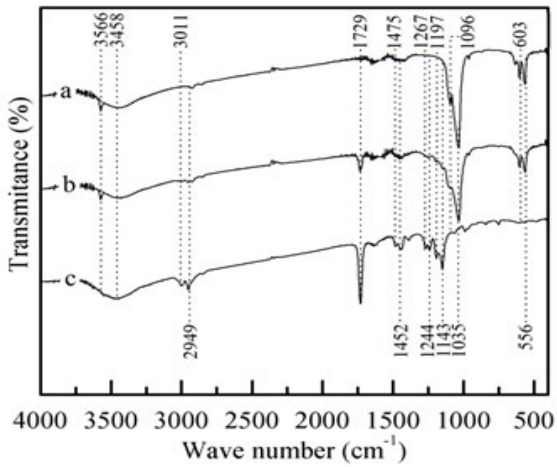

Fig. 2: FT-IR spectra of (a) Pure HA (b) PMMA-HA nanocomposite and (c) PMMA

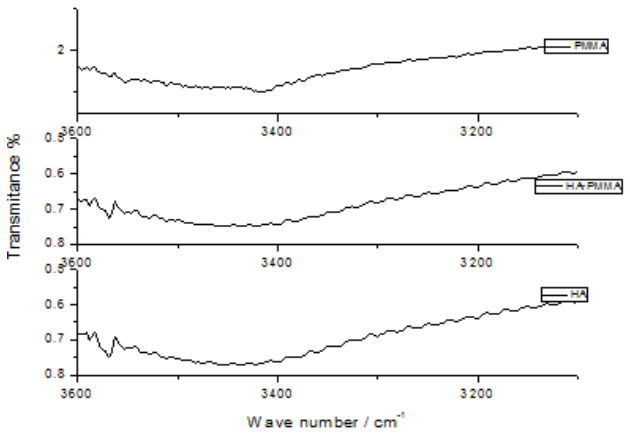

Fig. 3: FT-IR spectra of (a) Pure HA (b) PMMA-HA nanocomposite and (c) PMMA (expanded view from 3600 cm^{-1} to 3100 cm^{-1})

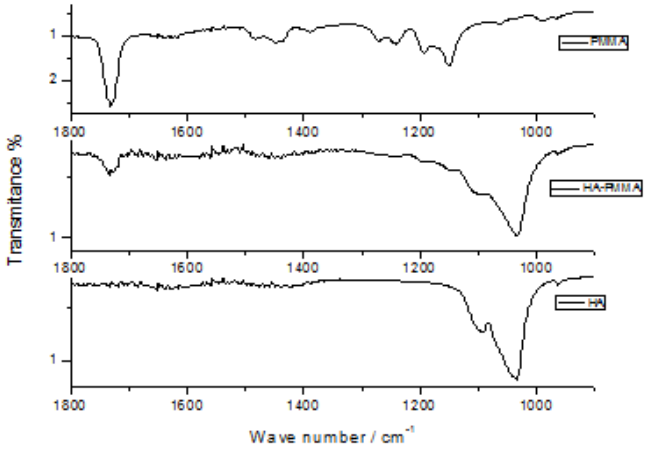

Fig. 4: FT-IR spectra of (a) Pure HA (b) PMMA-HA nanocomposite and (c) PMMA (expanded view from 1800 cm^{-1} to 900 cm^{-1})

Moreover, the vibrational band of C-O-C methoxy group of pure PMMA was shifted to 1145 cm^{-1} from 1147 cm^{-1}, indicating an interaction between the polymer and HA phase in the nanocomposite. Vibrational band of skeletal deformation of PMMA is not resolved in the spectrum of nanocomposite (Fig. 4). Further, the band position of skeletal C-C of PMMA appeared at the same place with a lower intensity in the spectrum of the nanocomposite (Fig. 4). Moreover, P-O stretching vibration bands of pure HA were shifted to 563 and 603 cm^{-1} in the spectrum of nanocomposite from 565 and 601 cm^{-1} respectively also indicating an interaction between HA and PMMA in the nanocomposite (Fig 6). Additionally, there was a significant shift in one of the stretching vibrational peaks of PO_4^{3-} in the formation of nanocomposite where the peak positions were shifted to 1031 and 1097 cm^{-1} from 1033 and 1097 cm^{-1} respectively. (Fig. 5) All of these results account for the indication of chemical interactions between HA and PMMA, most likely through the dipolar interactions of P of PO_4^{3-} exposed in the (010) plane with ester oxygen atoms of PMMA and also by H-bonding of surface hydroxyl groups of HA with the ester oxygen atoms of PMMA.

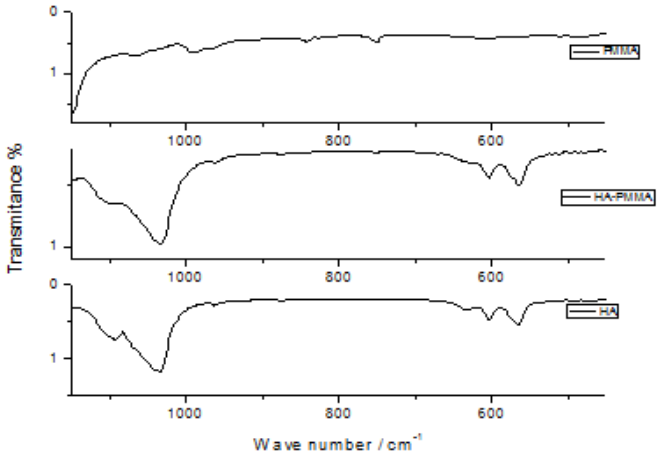

Fig. 5: FT-IR spectra of (a) Pure HA (b) PMMA-HA nanocomposite and (c) PMMA (expanded view from 1150 cm-1 to 450 cm^{-1})

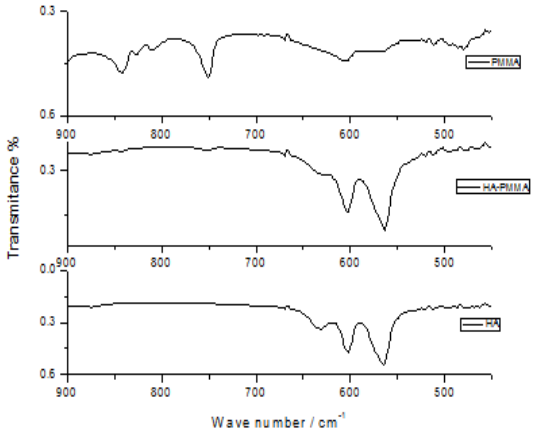

Fig. 6: FT-IR spectra of (a) Pure HA (b) PMMA-HA nanocomposite and (c) PMMA (expanded view from 900 cm-1 to 400 cm^{-1})

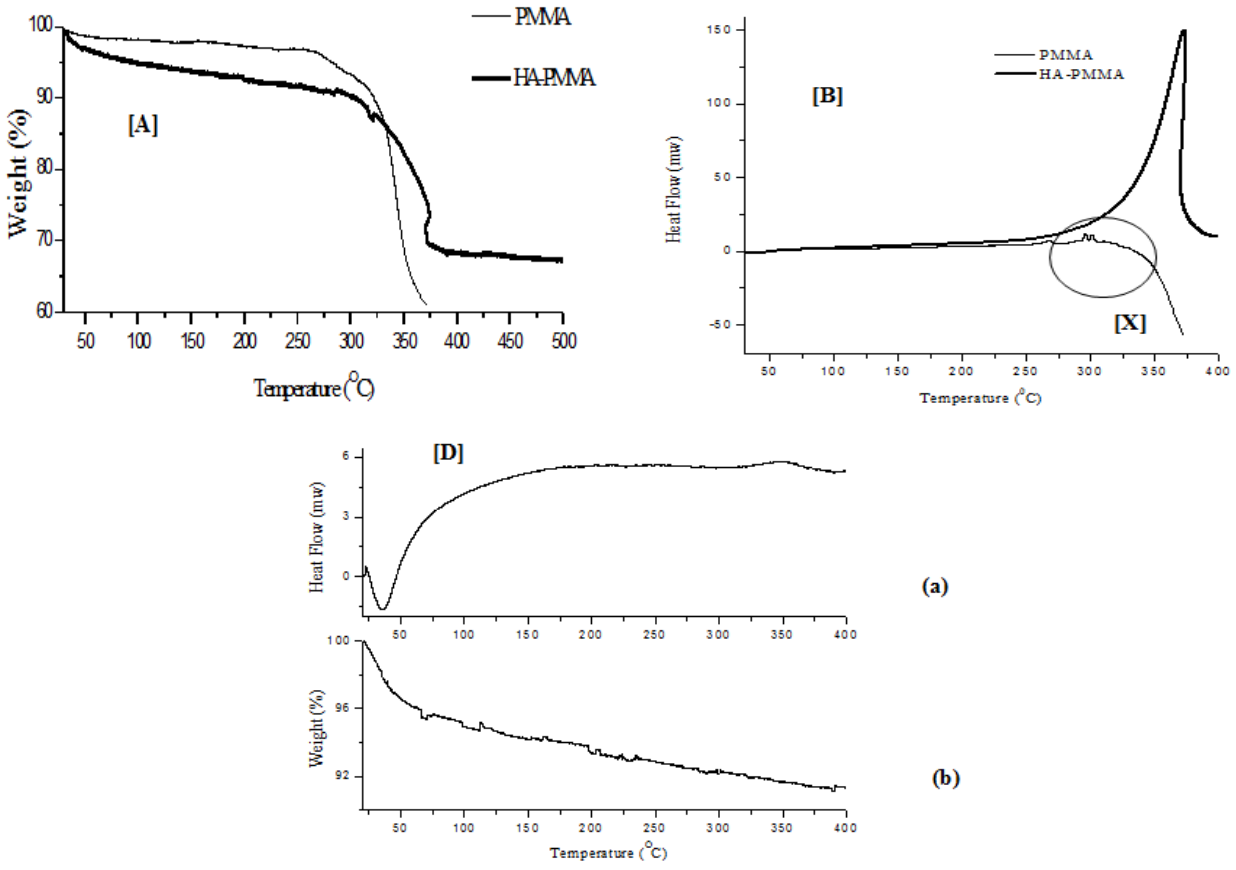

Fig. 7: [A] TGA curves of PMMA and PMMA-HA Nanocomposite, [B] DSC curves of PMMA and PMMA-HA Nanocomposite, and [C] (a) TGA and (b) DSC curves of HA.

In order to analyze the homogeneous distribution of polymer in the nanocomposite, randomly selected portions (5 mg) of the nanocomposite samples were analyzed by TGA and DSC.

TGA results indicate that water loss and the polymer loss at various locations were between 20 - 23% and 52-58% respectively (Table 2). It could be concluded, therefore, that the chemical composition of the nanocomposite is homogeneous and therefore, a good dispersion of nanoparticles in the PMMA matrix can be obtained in the synthesis of HA-PMMA nanocomposite when both HA and PMMA were produced simultaneously from Ca^{2+}, $PO_4$3-, and OH- sources and the monomer. In mature bone, HA nanocrystals are dispersed in the collagen matrix in a ratio of 69: 31, and according to TGA data in the synthetic analogue, average PMMA: HA ratio was 71: 29.

PMMA-HAp Sample	H_2O loss (wt%)	PMMA loss (wt%)	PMMA (wt%)	HA (wt%)
1	22.89	57.32	74	26
2	20.51	54.35	68	32
3	22.48	52.54	68	32
4	22.46	54.64	70	30

Table 2: Composition of HA-PMMA nanocomposite determined using TGA plots of the nanocomposites.

Colloidal apatite nanospheres of 2-5 nm in diameter was synthesized in the presence of poly(acrylic acid), PAA by San-Yuan Chen et al[35]. It is used as a structure directing agent for the synthesis of calcium-deficient apatite (CDHA). Experimental observation suggests that there exists a critical amount of the low-molecular-weight PAA, above which morphological evolution of CDHA nanoparticles from needle to sphere was observed. Balamurugan et al[36] attempted to develop a ceramic/polymer composite by grafting PMMA with HA by using suitable grafting agent (PMMA was coupled and grafted onto HA particles via covalent bonding of isocyanate groups of isocyanate ethyl methacrylate). The synthesized composite was characterized using spectral techniques. The present approach is quite different to these methods as both the polymer and the inorganic crystals are synthesized in situ in one pot. This approach provides nanocomposites with controlled physical and chemical properties.

Scanning Electron Microscopy (SEM)

Fig. 8 shows SEM images of HA, PMMA and the HA-PMMA composite. PMMA particles are in spherical shape in the average particle size of 200 nm. The HA particles in pure HA showed spherical shapes (Fig. 8(b)) and the PMMA-HA nanocomposite has become needle-shaped (Fig. 8(c)) and approximately in 10 nm X 50 nm dimensions, showing the effect of the polymer enforcing the nucleation and growth of HA particles. The space restrictions enforced by the polymer on the growing HA particles and their higher interactions in 'a' axis direction have made the particles more elongated in c axis direction than spherical. The possible primary growth of the mineral crystals is limited as the growth of apatite crystals of nanocomposite occurs within the polymer matrix. Thus the crystals are forced to be discrete and discontinuous. Homogeneous dispersion of HA in PMMA matrix (Fig. 8 (c) and (d)) shows that PMMA has played an important role in controlling the size and mono-dispersion of HA in nanoparticles. Similarly, the properties of bone are determined at the nanoscale level, with nanoapatite calcium phosphate crystals embedded in the soft collagen fibrils[38–40]. The collagen fibres, surrounded and infiltrated by the mineral are the most significant structures seen at hundreds of nanometers to 1 μm scale. The mature apatite crystals are not needle-shaped, but plate-shaped as the collagenous phase plays a central role in the regulation of mineralization, and the extent of mineral–collagen interactions[41,42]. Therefore in this work, the role of collagen in bones is tried to substitute by the role of PMMA as its well known clinical use with encouraging results in orthopaedic surgery for the fixation of artificial joints for last fifty years [43].

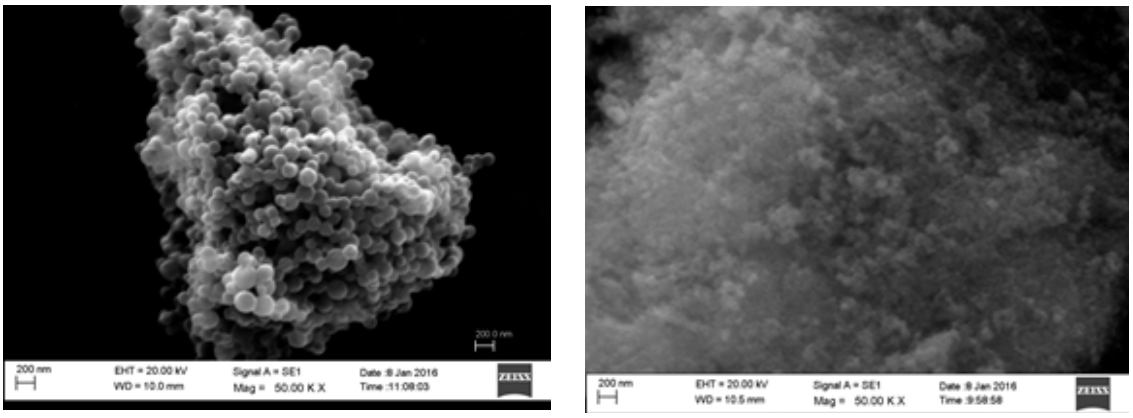

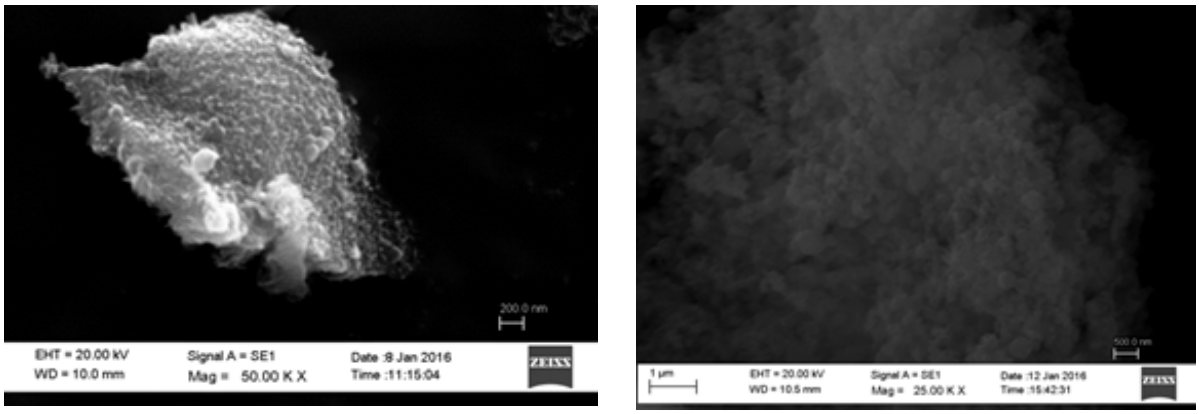

Fig. 8: SEM Image of (a) pure PMMA, (b) HA nanoparticles, and (c) HA-PMMA nanocomposite (d) HA-PMMA nanocomposite in a lower magnification

During the bottom-up approach, nano-HA and PMMA are allowed to self-assemble into an organized structure where freshly distilled MMA undergoes free radical vinyl polymerization using the heat-generated persulphate free radical and the simultaneous synthesis of HA nanoparticles through the combination of three stages: supersaturation, nucleation and crystal growth.

Flexural strength of cortical bone is between 50 – 150 MPa[41] but the value depends on the bone direction, longitudinal or transverse, and the bone location [39]. In the current study, the flexural strength of HA alone was 1.64 MPa and it was 5.51 MPa in the HA-PMMA nanocomposite. The value is comparable with the flexural strength of cancellous bone which is around 1-20 MPa [12,41]. The Young's modulus of cortical bone is reported to be around 7-25 GPa[12,44] and the synthetic analogue which has about 30% of HA mass percentage in the nanocomposite, has Young's modulus of 19 GPa and that of HA alone is 27 GPa. Although the natural hierarchical structure is difficult to achieve in the laboratory synthesis, the HA-PMMA nanocomposite described in this work has a similar Young's modulus in the range of cortical bone.

An excellent bone implant material should be able to rapidly induce osteogenesis and form tight bony bonds with host bone [45]. As the HA component of the nanocomposite has more similarity to the bone mineral in composition, crystal structure, crystallinity and morphology[39] better osteoconductivity for the nanocomposites is expected.

Conclusions

Homogeneous dispersion of needle shape, discrete, discontinuous, less crystalline HA nanoparticles (~29% of HA) in the PMMA matrix can be obtained by a novel method, one spot synthesis of in situ HA-PMMA nanocomposites using $Ca(OH)_2$, $NH_4H_2PO_4$ precursors, MMA monomers and $K_2S_2O_8$ initiator in a single container at 80°C without controlling the pH manually. HA nanoparticles were able to bond via non-covalent bonds in the PMMA matrix. Flexural strength of the nanocomposite was higher than that of pure HA which is having a comparable value of natural cancellous bone. However, Young's modulus of the nanocomposite was lower than that of pure HA, but the values are comparable with the value of natural cortical bone. In addition to the above properties, as there are enough clinical and experimental data supporting the performance of HA and PMMA, the nanocomposite can be used for the possible applications in bone grafting.

Acknowledgement

We acknowledge the Sri Lanka National Science Foundation for the financial support (Research Grant No: RG/2007/FR/08).

References

1. J. Wolff, The Law of Bone Remodeling, Springer-Verlag, Berlin, 1986.

2. M.M. Stevens, Biomaterials for bone tissue engineering, Mater. Today. 11 (2008) 18–25. doi:10.1016/S1369-7021(08)70086-5.

3. S. V. Dorozhkin, Calcium orthophosphate-based biocomposites and hybrid biomaterials, J. Mater. Sci. 44 (2009) 2343–2387.

4. Marı´a Vallet-Regı´ and Daniel Arcos, M. Vallet-Regı, D. Arcos, Biomimetic Nanoceramics in Clinical Use: From Materials to Applications, The Royal Society of Chemistry, Cambridge, UK, 2010. http://www.nanoarchive.org/7227/.

5. McConnell D., The crystal structure of bone, Clin Orthop Relat Res. 23 (1962) 253–68.

6. L.K.-S. and P.Z. J. Y. Rho, J.Y. Rho, L. Kuhn-Spearing, P. Zioupos, Mechanical properties and the hierarchical structure of bone, Med. Eng. Phys. 20 (1998) 92–102. doi:10.1016/S1350-4533(98)00007-1.

7. Currey J. D., Bones: structure and mechanics, Princeton University Press, New Jersey, 2002.

8. P. Turon, L.J. del Valle, C. Alemán, J. Puiggalí, Grafting of Hydroxyapatite for Biomedical Applications, in: Biopolym. Grafting Appl., Elsevier, 2018: pp. 45–80. doi:10.1016/B978-0-12-810462-0.00002-8.

9. Self-assembly, Nanotechnol. Encycl. (2016). www.edinformatics.com/nanotechnology/self_assembly.htm (accessed February 24, 2016).

10. B.J.R. and T.X. J. Kao, K. Thorkelsson, P. Bai, Toward functional nanocomposites: taking the best of nanoparticles, polymers and small molecules, Chem. Soc. Rev. 42 (2013) 2654–2678.

11. J. Wang, L. Wang, Y. Fan, Adverse Biological Effect of TiO 2 and Hydroxyapatite Nanoparticles Used in Bone Repair and Replacement, (2016) 1–14. doi:10.3390/ijms17060798.

12. a S. Brydone, D. Meek, S. Maclaine, Bone grafting, orthopaedic biomaterials, and the clinical need for bone engineering, Proc. Inst. Mech. Eng. Part H J. Eng. Med. 224 (2010) 1329–1343. doi:10.1243/09544119JEIM770.

13. V.K.G. Park, Sang-hyun, A. Llinas, J.C. Keller, Hard Tissue Replacements, in: J.D.B. J. B. Park (Ed.), Biomater. Princ. Appl., CRC

Press LLC, Boca Raton, 2003: pp. 173–192.

14. K. de G. Pamela Habibovic, Osteoinductive biomaterials – properties and relevance in bone repair, J. Tissue Eng. Regen. Med. 1 (2007) 25–32. doi:10.1002/term.

15. D. Zhang, X. Wu, J. Chen, K. Lin, The development of collagen based composite scaffolds for bone regeneration, Bioact. Mater. (2017). doi:10.1016/J.BIOACTMAT.2017.08.004.

16. M.E. Diken, S. Doğan, Y. Turhan, M. Doğan, Biological properties of PMMA/nHAp and PMMA/3-APT-nHAp nanocomposites, Int. J. Polym. Mater. Polym. Biomater. (2017) 1–9. doi:10.1080/00914037.2017.1378885.

17. M. Bayani, S. Torabi, A. Shahnaz, M. Pourali, Main properties of nanocrystalline hydroxyapatite as a bone graft material in treatment of periodontal defects. A review of literature, Biotechnol. Biotechnol. Equip. 31 (2017) 215–220. doi:10.1080/13102818.2017.1281760.

18. Salernitano E. and Migliaresi C., Composite materials for biomedical applications: a review, J. Appl. Biomater. Funct. Mater. 1 (2003) 3–18. doi:https://doi.org/10.1177/228080000300100102.

19. S.N.J. and M.J. Huang, J., S.M. Best, W. Bonfield, R.A. Brooks, N. Rushton, Edirisinghe, In vitro assessment of the biological response to nano-sized hydroxyapatite., J. Mater. Sci. Mater. Med. 15 (2004) 441–445.

20. M.H. Fathi, A. Hanifi, V. Mortazavi, Preparation and bioactivity evaluation of bone-like hydroxyapatite nanopowder, J. Mater. Process. Technol. 202 (2008) 536–542. doi:10.1016/j.jmatprotec.2007.10.004.

21. S.C.J. Loo, T. Moore, B. Banik, F. Alexis, Biomedical applications of hydroxyapatite nanoparticles., Curr. Pharm. Biotechnol. 11 (2010) 333–342. doi:10.2174/138920110791233343.

22. M. Manoj, R. Subbiah, D. Mangalaraj, N. Ponpandian, C. Viswanathan, K. Park, Influence of Growth Parameters on the Formation of Hydroxyapatite (HAp) Nanostructures and Their Cell Viability Studies, (2015) 1–11. doi:10.5772/60116.

23. S. Shinzato, T. Nakamura, T. Kokubo, Y. Kitamura, PMMA-based bioactive cement: Effect of glass bead filler content and histological change with time, J. Biomed. Mater. Res. 59 (2002) 225–232. doi:10.1002/jbm.1236.

24. H. Sun, C. Liu, H. Liu, Y. Bai, Z. Zhang, X. Li, C. Li, H. Yang, L. Yang, A novel injectable calcium phosphate-based nanocomposite for the augmentation of cannulated pedicle-screw fixation., Int. J. Nanomedicine. 12 (2017) 3395–3406. doi:10.2147/IJN.S131962.

25. C. Knoell, A., Maxwell, H., and Bechtol, Graphite fiber reinforced bone cement., Ann. Biomed. Eng. 3 (1975) 225–229.

26. J.M. Topoleski, L. D. T., Ducheyne, P., and Cackler, The fracture toughness of titanium fiber reinforced bone cement., J. Biomed. Mater. Res. 26 (1992) 1599–1617.

27. R.S. Lakes, Composite Biomaterials, in: J.D.B. J. B. Park (Ed.), Biomater. Princ. Appl., CRC Press LLC, Boca Raton, 2003: pp. 79–91.

28. T. Shokuhfar, A. Makradi, E. Titus, G. Cabral, S. Ahzi, A.C.M. Sousa, S. Belouettar, J. Gracio, Prediction of the mechanical properties of hydroxyapatite/polymethyl methacrylate/carbon nanotubes nanocomposite., J. Nanosci. Nanotechnol. 8 (2008) 4279–4284. doi:10.1166/jnn.2008.AN26.

29. V.S. and S.R. A. Balamurugan, S. Kannan, a Balamurugan, S. Kannan, V. Selvaraj, S. Rajeswari, Development and Spectral Characterization of Poly(Methyl Methacrylate) /Hydroxyapatite Composite for Biomedical Applications, Trends Biomater. Artif. Organs. 18 (2004) 41–45.

30. K.A. Bhat, P. Leo Prakash, N. Manoharan, A. Lakshmibai, D. Sangeetha, Fabrication of polymethyl methacrylate/polysulfone/nanoceramic composites for orthopedic applications, J. Appl. Polym. Sci. 127 (2013) 2764–2775. doi:10.1002/app.37581.

31. P.M. Chou, M. Mariatti, The Properties of Polymethyl Methacrylate (PMMA) Bone Cement Filled with Titania and Hydroxyapatite Fillers, Polym. Plast. Technol. Eng. 49 (2010) 1163–1171. doi:10.1080/03602559.2010.496403.

32. P. Monvisade, P. Siriphannon, R. Jermsungnern, S. Rattanabodee, Preparation of hydroxyapatite/poly(methyl methacrylate) and calcium silicate/poly(methyl methacrylate) interpenetrating hybrid composites, J. Mater. Sci. Mater. Med. 18 (2007) 1955–1959. doi:10.1007/s10856-007-3142-2.

33. Pelfrey, S., Cantu, T., Papantonakis, M.R., Simonson D.L., McGill R.A., and Macossay, J., Microscopic and spectroscopic studies of thermally enhanced electrospun PMMA micro- and nanofibers., Polym. Chem. 1 (2010) 866–869.

34. Mbese, J.Z., and Ajibade P.A., Preparation and characterization of ZnS, CdS and HgS/Poly(methyl methacrylate) Nanocomposites., Polymers (Basel). 6 (2014) 2332–2344.

35. S.C. Liou, S.Y. Chen, D.M. Liu, Manipulation of nanoneedle and nanosphere apatite/poly (acrylic acid) nanocomposites, J. Biomed. Mater. Res. - Part B Appl. Biomater. 73 (2005) 117–122. doi:10.1002/jbm.b.30193.

36. a Balamurugan, S. Kannan, V. Selvaraj, S. Rajeswari, Development and Spectral Characterization of Poly(Methyl Methacrylate)/Hydroxyapatite Composite for Biomedical Applications, Anal. Chem. 18 (2004) 41–45.

37. V. M. Parikh, Absorption spectroscopy of organic molecules, Addison-Wesley publishing company, 1996.

38. A.C. and Lawson, J.T. Czernuszka, Collagen – calcium phosphate composites, Proc Instn Mech Engrs. 212 (n.d.) 413–425.

39. R. Murugan, S. Ramakrishna, Development of nanocomposites for bone grafting, Compos. Sci. Technol. 65 (2005) 2385–2406. doi:10.1016/j.compscitech.2005.07.022.

40. N. Nassif, F. Gobeaux, J. Seto, E. Belamie, P. Davidson, P. Panine, G. Mosser, P. Fratzl, M.M. Giraud Guille, Self-assembled collagen-apatite matrix with bone-like hierarchy, Chem. Mater. 22 (2010) 3307–3309. doi:10.1021/cm903594n.

41. S. Bandyopadyay-Ghosh, Bone as a collagen-hydroxyapatite composite and its repair, Trends Biomater. Artif. Organs. 22 (2008) 112–120.

42. S. Weiner, W. Traub, Bone structure: from angstroms to microns., FASEB J. 6 (1992) 879–885.

43. J. Charnley, Anchorage of the femoral head prosthesis to shaft of the femur, J. Bone Jt. Surg. 42B (1960) 28–35.

44. M. Nordin and V. H. Frankel, Basic biomechanics of the muscle skeletal system, Lippincott Williams and Wilkins. (2001) 35.

45. W.C. Deng X, Hao J, Preparation and mechanical properties of nanocomposites of poly(D,L-lactide) with Ca-deficient hydroxyapatite nanocrystals., Biomaterials. 22 (2001) 2867–73.